Process Safety and Environmental Protection 149 (2021) 244–257

Contents lists available at ScienceDirect

Process Safety and Environmental Protection

journal homepage: www.elsevier.com/locate/psep

Effect of interfaces on gas breakthrough pressure in compacted bentonite used as engineered barrier for radioactive waste disposal

Vanesa Gutiérrez-Rodrigo, Pedro Luis Martín, María Victoria Villar*

Centro de Investigaciones Energéticas, Medioambientales y Tecnológicas (CIEMAT), Avd. Complutense 40, 28040, Madrid, Spain

ARTICLE INFO

Article history:
Received 28 July 2020
Received in revised form
29 September 2020
Accepted 30 October 2020
Available online 4 November 2020

Keywords:
Bentonite
Gas transport
Engineered barrier
Saturation
Porosity
Interface

ABSTRACT

In a deep geological nuclear waste repository gas can be generated by different processes. Understanding the gas transport mechanisms across the engineered and natural barriers in a repository is relevant for its security assessment, both in terms of mechanical stability and of radionuclide transport. The engineered barrier may be composed of compacted blocks of bentonite and the interfaces between these blocks might evolve into preferential fluid pathways, in particular for the gas generated around the waste canisters. Small-scale laboratory tests were performed in sound samples and in samples crossed by an interface to determine gas breakthrough pressure values after saturation and the effect on them of the interface. The FEBEX bentonite, a Spanish bentonite composed mainly of montmorillonite, was used in the tests. The gas breakthrough pressure of the saturated compacted samples increased with dry density and was higher than the swelling pressure of the bentonite. Gas breakthrough could take place either in an instantaneous or in a gradual way, the difference between both modes being the flow rate, much higher in the first case. The gas transport mechanism would be microscopic pathway dilation, with microfracturing in the case of the instantaneous episodes. A sealed interface along the bentonite did not seem to affect the breakthrough pressure or gas permeability values, since the behaviour patterns were similar in both kinds of samples, depending mostly on the bentonite dry density.

1. Introduction

Geological disposal is the preferred, internationally accepted option for wastes with high levels of radioactivity. The concept considers the excavation of repositories at depths of several hundred of metres in suitable host rocks with a series of barriers between the waste and the surface acting in concert to contain the wastes as shown in Fig. 1 (e.g. Chapman and McCombie, 2003; Ewing et al., 2016). Bentonites or bentonite-based materials have frequently been proposed to construct the buffer around the waste container –one of the engineered barriers– because of their high chemical retention capacity, high swelling ability and low permeability (e.g. Pusch, 1994; Cuadros, 2008; Sellin and Leupin, 2013).

The heat released by the waste will induce a thermal gradient through the bentonite barrier, while groundwater will tend to flow into it. As a consequence, coupled thermal, hydraulic, mechanical and geochemical processes will take place during the transient period of the repository life, when the temperature is high and the barrier is slowly hydrating until reaching full saturation (e.g. Gens et al., 2009). Additionally, gas will be generated within the repository by several mechanisms, in particular the anaerobic corrosion of metals (such as the waste canisters), the microbial degradation of organic wastes and the radiolysis of water, which generate hydrogen, oxygen, methane and carbon dioxide.

To assess the performance of a deep geological repository as a whole (waste, engineered barrier, excavation disturbed zone, host rock) and, in particular, its gas transport properties, understanding gas generation and migration is vital. The gas pressure could rise and build up if the generation rates are higher than the rate by which gas is transported away within the repository. When the pressure of the accumulated gas reaches the breakthrough value, the repository structure and properties might be affected and contaminated water driven into the geosphere (e.g. Rodwell et al., 1999; Johnson, 2006).

Gas migration in saturated compacted bentonite observed in laboratory tests is generally interpreted as occurring by the formation and propagation of dilatant pathways within the bentonite (e.g. Pusch and Forsberg, 1983; Gallé and Tanai, 1998; Horseman et al., 1999; Harrington and Horseman, 1999; Gallé, 2000; Harrington and Horseman, 2003; Olivella and Alonso, 2008). This gas transport mechanism implies that there is no water displacement resulting from gas entry into the clay or measurable desaturation of

* Corresponding author.
E-mail address: mv.villar@ciemat.es (M.V. Villar).

https://doi.org/10.1016/j.psep.2020.10.053

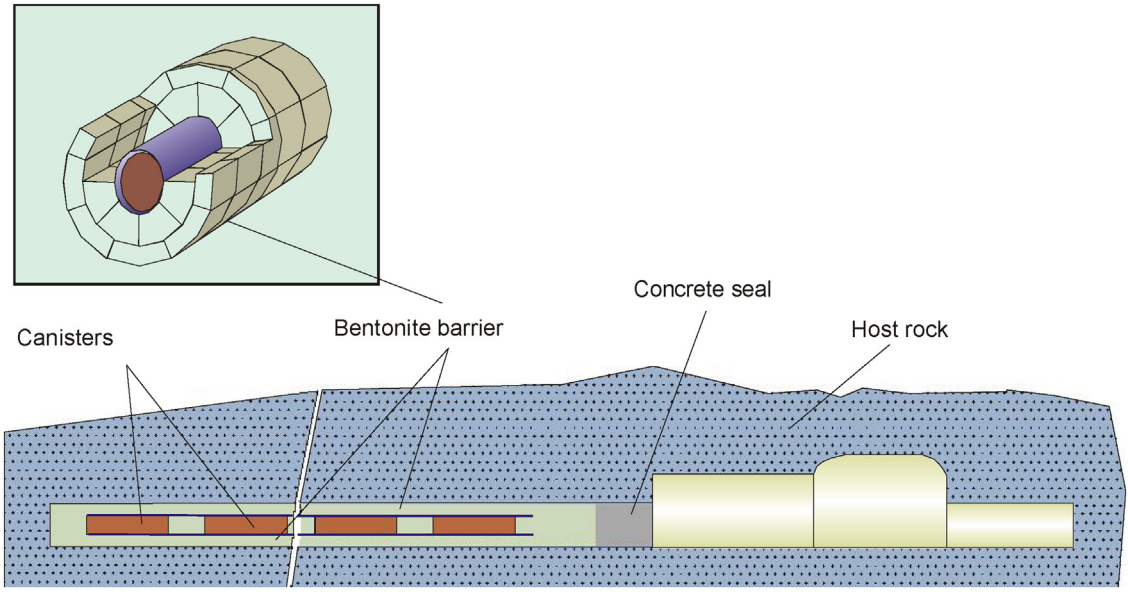

Fig. 1. Schematic design of a generic deep geological repository concept for nuclear waste, with the bentonite barrier around the waste canisters (ENRESA, 1995).

the samples. Dilatant pathways are also revealed by the strong coupling between the stress state of the sample and the pressure required for gas to enter the clay, the local changes in stresses and the unstable flow (Graham et al., 2016). The 'gas breakthrough pressure' is the critical threshold pressure above which gas outflow is observed at the downstream end of a sample across which a pressure gradient is applied (Graham et al., 2016). Evidence of fissure opening by air injection in an argillaceous rock (the Cenozoic Boom Clay) was detected and analysed by mercury intrusion porosimetry and X-ray micro-computed tomography (González-Blanco et al. 2017). Xu et al. (2015) concluded that gas migration in saturated soft clay was influenced by the capillary pressure and the mechanical stress simultaneously. In this sense they defined two key parameters: the gas entry pressure and the gas induced-dilatancy pressure, referring to the capillary pressure and the mechanical stress effects, respectively. They considered that the sudden increase of gas flux under high gas injection pressures could be caused by the mechanically-induced dilatancy of channels, capillary pressure-induced continuous flow pathways, as well as the failure of sealing-efficiency.

Harrington et al. (2017) observed in compacted saturated bentonite multiple discrete gas propagation events, affected by spatial variability and time dependency. They described perturbations of the stress field before gas outflow occurred that reduced as steady-state was approached. According to these authors, gas would penetrate by generating microfractures: breaking the bonds between the water and the clay and compressing the surrounding clay matrix, which resulted in localised consolidation.

The knowledge of the movement of gases through the repository structure is required to determine the magnitude of these effects and the need to accommodate them in the repository design and safety calculations. This was the focus of the research in the integrated, multidisciplinary project FORGE (2009–2013, https://www.bgs.ac.uk/forge/), during which part of the results presented here were obtained (Shaw, 2015). Built on the outcomes of FORGE, a project on the understanding and predictability of gas migration in natural and engineered clay materials has been fostered by the European Union (EURAD-WP6 GAS, 2019–2024), since increasing the understanding of gas migration is considered a high priority topic, in particular answering the questions about how gas can migrate within the repository and which water soluble and volatile radionuclides could be associated with it, and to what extend could the hydro-mechanical perturbations induced by gas affect barrier integrity and performance (https://www.ejp-eurad.eu/implementation/mechanistic-understanding-gas-transport-clay-materials-gas).

The buffer of a repository may be constructed from compacted clay blocks of different sizes and shapes (Fig. 1). In this respect, the behaviour of an engineered barrier system will be determined not only by the matrix properties of the sealing material, but by the interfaces between the different elements of the sealing system, in particular the interfaces between the clay blocks or between the clay barrier and the host rock. These interfaces may act not only as mechanical weakness planes, but also as preferential gas pathways. For instance, despite the assumed self-sealing capacity of bentonite, inherent existing interfaces might be reopened during gas injection (Popp et al., 2014). However, these authors confirmed the complete healing of the interface between blocks of a bentonite/sand (60/40) mixture after saturation. Self-healing processes can be viewed as sealing with a loss of memory of the pre-sealing state (in this case, the interface prior to saturation), and may involve geochemical processes (Davies and Bernier, 2004). In contrast, Davy et al. (2009) analysed in laboratory tests the bentonite/argillite interface, and concluded that, although the assemblage formed by the two materials was highly impermeable to water (i.e. the interface sealed well after saturation), gas leakage would occur preferentially along this interface if the gas pressure was sufficiently increased (i.e. the interface did not heal). However, from the results of a series of similar tests, Liu (2012) was not able to ascertain if the gas moved along the bentonite/argillite interface or across the argillite, whose breakthrough pressures are lower than those of bentonite.

The experimental work presented here aimed to understand the gas transport in a saturated clay barrier, i.e. the behaviour at a stage in the repository life in which groundwater inflow has completely saturated the barrier and the gas generation processes have started to be active and relevant. The tests were designed to determine the gas breakthrough pressure and additionally estimate a permeability value once breakthrough occurred (Villar et al., 2013; Gutiérrez-Rodrigo et al., 2015; Gutiérrez-Rodrigo, 2018). The role of interfaces inside the bentonite barrier, i.e. between compacted bentonite blocks, was also tested (with preliminary results presented in Gutiérrez-Rodrigo et al., 2015).

To the authors' knowledge, this is the first published systematic study of the effect of bentonite dry density on breakthrough pressure, covering a large range of densities selected considering the expected range of variation in the bentonite barrier (ENRESA 2006). Additionally, there are no other results reported on the role of interfaces between compacted bentonite on gas transport.

2. Material and methods

2.1. Material: the FEBEX bentonite

The material FEBEX bentonite was extracted from the Cortijo de Archidona deposit (Almería, Spain). At the factory, the clay was disaggregated and gently dried to a water content of around 14 %, all the material of particle size greater than 5 mm being rejected. The physico-chemical properties of the FEBEX bentonite, as well as its most relevant thermo-hydro-mechanical and geochemical characteristics are reported in ENRESA (2006) and Villar and Gómez-Espina (2009) and summarised below.

The smectite content of the FEBEX bentonite is above 90 wt.%. The smectitic phases are actually made up of a montmorillonite-illite mixed layer, with 10–15 wt.% of illite layers. Besides, the bentonite contains variable quantities of quartz, plagioclase, K-felspar, calcite, and cristobalite-trydimite. The cation exchange capacity of the smectite is 102 ± 4 meq/100 g, the main exchangeable cations being calcium (35 ± 2 meq/100 g), magnesium (31 ± 3 meq/100 g) and sodium (27 ± 1 meq/100 g). The predominant soluble ions are chloride, sulphate, bicarbonate and sodium.

The liquid limit of the bentonite is 102 ± 4 %, the plastic limit 53 ± 3 %, the density of the solid particles 2.70 ± 0.04 g/cm^3, and 67 ± 3 % of particles are smaller than 2 μm. The hygroscopic water content in equilibrium with the laboratory atmosphere (relative humidity 50 ± 10 %, temperature 21 ± 3 °C) is 13.7 ± 1.3 %. The external specific surface area is 32 ± 3 m^2/g and the total specific surface area is about 725 ± 47 m^2/g.

The saturated hydraulic conductivity of compacted samples of the FEBEX reference bentonite is exponentially related to their dry density. The empirical relationship between hydraulic conductivity (k_w, m/s) and dry density (ρ_d, g/cm^3) shown in Eq. 1 was obtained for samples compacted to dry densities above 1.47 g/cm^3 and in Eq. 2 for dry densities below that value. Both relationships were obtained from tests in which the samples were permeated with deionised water at room temperature. The deviation with respect to the theoretical values obtained with these equations was of ±30 %.

$$((1))\log k_w = -2.96\rho_d - 8.57$$

$$\log k_w = -6.00\rho_d - 4.09 \quad (2)$$

The swelling pressure (P_s, MPa) of compacted samples is also exponentially related to the bentonite dry density (ρ_d, g/cm^3), according to the empirical expression in Eq. 3, which indicates that when the bentonite at dry density of 1.6 g/cm^3 is saturated under constant volume with deionised water at room temperature, the swelling pressure has a value of about 6 MPa:

$$\ln P_s = 6.77\rho_d - 9.07 \quad (3)$$

The gas effective permeability of samples of FEBEX bentonite compacted to different dry densities with various water contents was measured in triaxial cells under confining pressures of 0.6 and 1.0 MPa (Villar et al., 2013). The gas permeability values obtained were related to the accessible void ratio (e ($1 - S_r$), with e being void ratio and S_r degree of saturation) through

$$k_{ig} \cdot k_{rg} = 1.25 \cdot 10^{-12} (e(1 - S_r))^{3.22} \quad (4)$$

2.2. Experimental setup

A series of stainless steel cells were designed and manufactured to perform gas breakthrough tests in saturated bentonite (Villar et al., 2013; Gutiérrez-Rodrigo et al., 2015). Isochoric cells were preferred over more conventional triaxial cells because of the difficulty in keeping the volume of expansive materials constant under triaxial conditions. The cells consisted of a body, pistons with o-rings at both ends of the samples and threaded caps (Fig. 2, left). The setup designed to measure breakthrough pressure (Fig. 2, right) consisted of two stainless steel airtight cylinders (75 cm^3, 124 bar) connected through valves to the ends of the cell and equipped with pressure transmitters (inlet pressure 135 bar a, outlet pressure 70 bar a, accuracy ±0.04 % FS, over pressure 4 x FS).

2.3. Preparation of samples

The samples, of 3.8 or 5.0 cm in diameter and 2.0 or 5.0 cm in height, were obtained by uniaxial compaction inside the cell body of the bentonite with its hygroscopic water content to dry densities between 1.4 and 1.8 g/cm^3. The same kind of tests was performed in sound samples and in samples with an interface, in order to check how effectively joints between bentonite blocks were sealed during the saturation process. The samples for tests on bentonite interfaces were prepared by uniaxially compacting cylindrical specimens that were later longitudinally cut with a saw (Fig. 3). After cutting the cylinders, the halves were put together inside the stainless steel cells shown in Fig. 2 with geotextile on top and bottom. The cutting process implied mass loss, and consequently a reduction in overall dry density with respect to the compaction value.

The cells used had smooth internal surfaces, but one of the tests was performed in a cell whose internal surface had been grooved, following a design first proposed by Liu (2013) and Liu et al. (2014). The aim of this design was to check the role of the interface between the bentonite and the stainless steel in gas transport.

2.4. Testing methodology

Prior to the gas transport tests, the bentonite was completely saturated with deionised water in the non-deformable steel cylindrical cells applying injection pressures of 0.2–0.6-0.8 MPa initially on one side and then on both (Phase 1). The saturation period lasted between 79 and 851 days, depending on the sample dry density and size and the equipment availability to move on to next phase. Once saturation was achieved, the filters through which saturation occurred were removed and replaced by dry stainless-steel filters before moving the cells to the setup shown in Fig. 2 (right), in which both sides of the cells were connected to gas cylinders equipped with pressure transducers (Phase 2). The swelling of the bentonite upon saturation was considered enough to ensure that gas did not flow between the bentonite and the cell wall. The samples were subjected to progressively higher pressures at one of their ends. An initial pressure of 400 kPa was fixed in the upstream cylinder, while a vacuum of 1 kPa-a was applied to the downstream cylinder (Fig. 2). The pressure in the upstream cylinder was increased every 24 h by 200 kPa until breakthrough occurred. The opposite-end cylinder recorded the pressure increase after gas broke through the sample. The time period every pressure step lasted was kept short to avoid a significant contribution of diffusion to gas transport. The moment gas suddenly crosses the saturated material is called "breakthrough" and "breakthrough pressure" is the necessary pressure to achieve this, which equals the pressure difference between both cylinders at that moment. Once gas flow stopped and

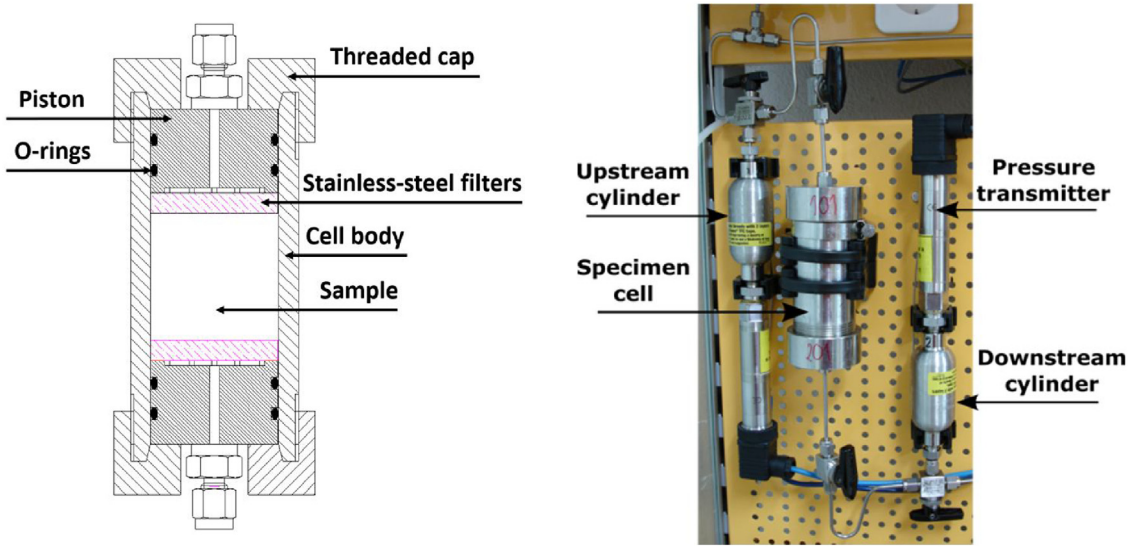

Fig. 2. Schematic design of the cells tests (left) and setup for breakthrough tests (right).

Fig. 3. Appearance of samples prepared for interface testing prior to saturation (sample JB1.6_38).

the pressure values in both cylinders were balanced, reaching what is called residual pressure, a pressure difference was applied again between both cylinders, in order to check material integrity after breakthrough, which would be proved if the same pressure difference was needed for the gas to cross again the sample. To this aim the pressure in the downstream cylinder was decreased every 24 h by 200 kPa until null pressure, and if flow did not occur, the pressure in the upstream cylinder was increased following the previous procedure. Once a new breakthrough episode took place, the pressures in the two cylinders were let stabilise again. The process of changing pressure either in the upstream or the downstream cylinders was sometimes repeated for a third time, which allowed to obtain three subsequent breakthrough episodes (not analysed here). After flow stopped, the cells were removed from the setup, weighed and measured and set for resaturation under the same conditions of Phase 1 (Phase 3). The saturation periods of Phase 3 lasted between 54 and 307 days. Finally, the cells were moved again to the gas breakthrough setup and the procedure to determine breakthrough pressure was repeated (Phase 4), triggering two new consecutive breakthrough episodes by changing the pressures in the upstream and downstream deposits as explained for Phase 2. Phases 3 and 4 were performed to check if the gas pathways opened during the first breakthrough test (Phase 2) were healed during resaturation.

Nitrogen gas was used for the breakthrough pressure determination, and the pressure in both cylinders was measured by means of pressure transducers. There was no further water supply once the gas pressures started to be applied.

2.5. Gas permeability computation

After breakthrough the flow of gas under the imposed pressure gradient could be estimated from the decay of the pressure difference across the sample with elapsed time, as in a variable head permeameter. An indirect method was used to determine the volumetric flow rate entering or exiting the sample (Loosveldt et al., 2002). The mean volumetric flow rate Q_m, where the subscript 'm' refers to reference conditions of T and P under which the mass flow was measured, was calculated as:

$$Q_m = V_v \times \left(\frac{\Delta\rho}{\rho}\right) \times \frac{1}{\Delta t} \quad (5)$$

where V_v is the volume of the cylinder (upstream or downstream, 50 or 75 cm^3), $\Delta\rho/\rho$ is the relative change in gas density, and Δt is the time interval in which the change in gas density took place. Taking into account the equation of state for real gases and considering that the tests were isothermal, the following relation can be obtained (Gutiérrez-Rodrigo et al., 2015; Gutiérrez-Rodrigo, 2018):

$$Q_m = V_v \times \left(\frac{\Delta P}{P_{av}}\right) \times \frac{1}{\Delta t} \quad (6)$$

where V_v is the volume of the cylinder, ΔP is the pressure change and P_{av} is the average pressure (upstream or downstream) in the cylinder (inlet or outlet) during the time interval considered.

The computation of permeability (intrinsic permeability measured with gas flow, k_{ig} (m^2), multiplied by the relative

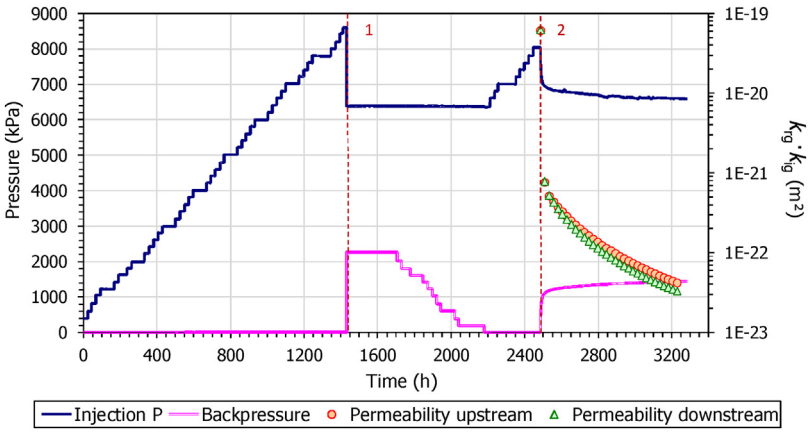

Fig. 4. Gas pressure evolution in the upstream and downstream cylinders during Phase 2 of test BT18_38 and effective gas permeability computed from the pressure changes in both cylinders.

permeability to gas, k_{rg}) from the pressure change was performed by applying the following Equation for incompressible media with compressible pore fluids (Scheidegger, 1974):

$$k_{ig} \cdot k_{rg} = [V_v]_{up,dw} \times \left(\frac{\Delta P}{P_{av}}\right)_{up,dw} \times \frac{1}{\Delta t} \times \frac{\mu_g \times L \times 2\,P_m}{A \times (P_{up}^2 - P_{dw}^2)} \qquad ((7))$$

where A (m^2) is the sample surface area, μ_g (Pa·s) is the fluid dynamic viscosity, L (m) is the sample length and P_{up} and P_{dw} (kPa) are the upstream and downstream pressures applied at the top (inlet) and the bottom (outlet), respectively, of the sample, and P_m (kPa) is the pressure of the measured flow. In this kind of tests the pressure of the measurement P_m (kPa) and the average pressure of the interval P_{av} (kPa) are the same.

The accuracy of this analysis depends on the assumptions that the pressure change was small or the gas behaved as an ideal gas and that a pseudo-steady state mass-flow was established, *i.e.* that the quantity of gas exiting the high pressure cylinder was approximately equal to that entering the low pressure cylinder.

2.6. Final determinations

The measurement of sample height and weighing of the cell after each phase allowed to compute intermediate values of dry density and water content. These were checked at the end of the tests, when the bentonite specimens, once extracted from the cells, were measured and weighed and the water content and dry density at three different levels (two, if they were 2-cm long) along the cylindrical specimens were determined. To determine the dry mass of the samples they were oven-dried at 110 °C for 48 h, and to compute the dry density, the volume of the same specimens was determined by immersing them in mercury prior to drying. Pore size distribution by mercury intrusion was also determined in many of the samples, but the results obtained are reported elsewhere (Gutiérrez-Rodrigo, 2018).

3. Results

A total of 15 breakthrough tests in sound samples and 5 in samples with interface was performed (Gutiérrez-Rodrigo, 2018). The results of 7 of the former and 2 of the latter were presented in Gutiérrez-Rodrigo et al. (2015), but for completeness are included here again. Additionally, the results of a test performed in a cell with grooved wall are presented. The reference given to each test includes: 1) the type of test (BT: breakthough in sound sample; JB: breakthrough in sample with interface), 2) the dry density, 3) the sample diameter, 4) the sample height (only indicated when it was not 5 cm). A summary of the main trends found in the whole set of tests is given here, with a focus on the differences between sound samples and samples with interface.

3.1. Breakthrough process

After saturation and resaturation of the samples (Phases 1 and 3, respectively), Phases 2 and 4 of the tests consisted in increasing stepwise the gas injection pressure (200 kPa every 24 h) in the upstream cylinder whereas the downstream cylinder was kept under close to vacuum conditions (~1 kPa). Although vacuum was initially applied in the downstream cylinder, as soon as the valve separating this cylinder from the sample cell was open, pressure increased to 2.5 kPa, which was caused by the sample water evaporation until vapour equilibrium at the test temperature was reached (~20 °C). For a 75-cm^3 cylinder, around 2 mg of water would be necessary. An example of the complete Phase 2 of one of the tests in sound samples is shown in Fig. 4 and of the Phase 4 of a test in a sample with interface in Fig. 5. The injection pressure was increased until breakthrough occurred, which corresponded to the moment in which pressure started to increase in the downstream cylinder, with a simultaneous decrease in the upstream cylinder (number 1 in Figs. 4 and 5), since the system was closed and there was no further gas supply between steps. When pressures in the two cylinders kept constant over time, indicating a no gas-flow condition, i.e. the shut-in of the clay, a new breakthrough was attempted by decreasing the pressure in the downstream cylinder (200 kPa every 24 h), so that to increase the pressure gradient. If the minimum pressure was reached and no breakthrough took place, the pressure in the upstream cylinder was again increased as initially until breakthrough was triggered for a second time (number 2 in Fig. 4). The test finished when the pressure in the two cylinders stabilised again. The fact that the gas pressure changed in the cylinders implied that there was gas flow, and permeability could be calculated as explained in section 2.5.

The breakthrough episodes were classified in instantaneous, when the gas flow stabilisation time once gas crossed the sample was shorter than one hour, and gradual (more frequently), when this time was longer. Gradual episodes corresponded to small gas flow rates during long time periods, flow stopping once the pressure difference between the two cylinders reached the residual pressure value (Figs. 4 and 5). The residual pressure is the pressure difference between the two cylinders once the pressures stabilised after breakthrough. Occasionally some pathways remained open and the equalisation of the pressure in both cylinders was reached (Fig. 6).

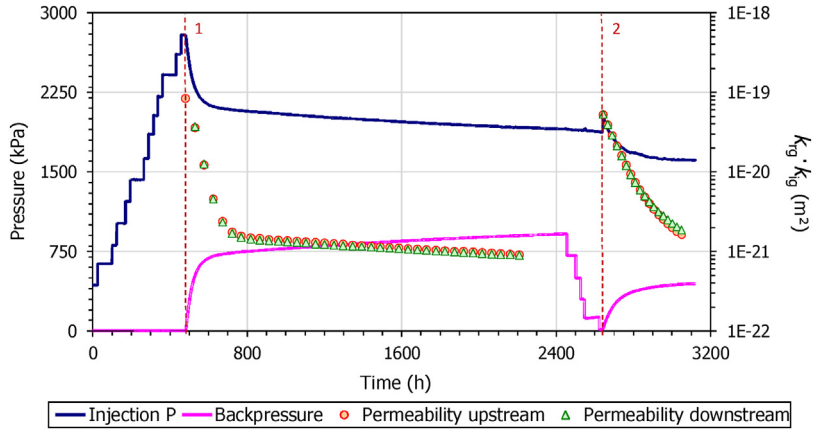

Fig. 5. Gas pressure evolution in the upstream and downstream cylinders during Phase 4 of test JB1.7_38 and effective gas permeability computed from the pressure changes in both cylinders.

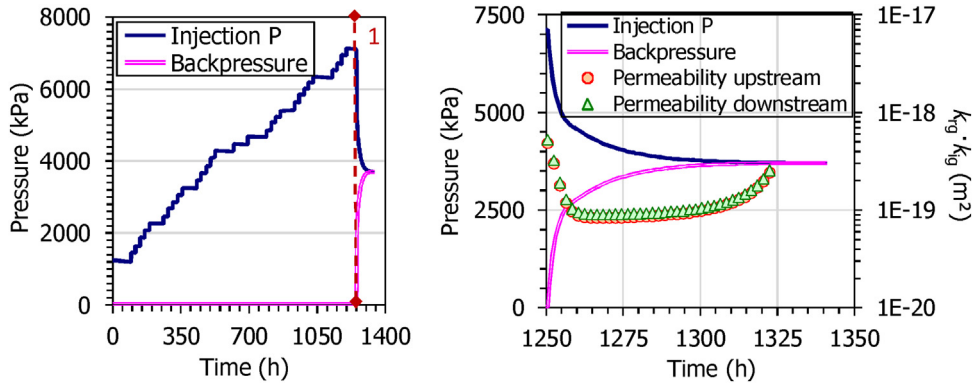

Fig. 6. Gas pressure evolution in the upstream and downstream cylinders during Phase 2 of test BT1.5_50. The figure on the right shows only the pressure changes after breakthrough and the effective gas permeability computed from them.

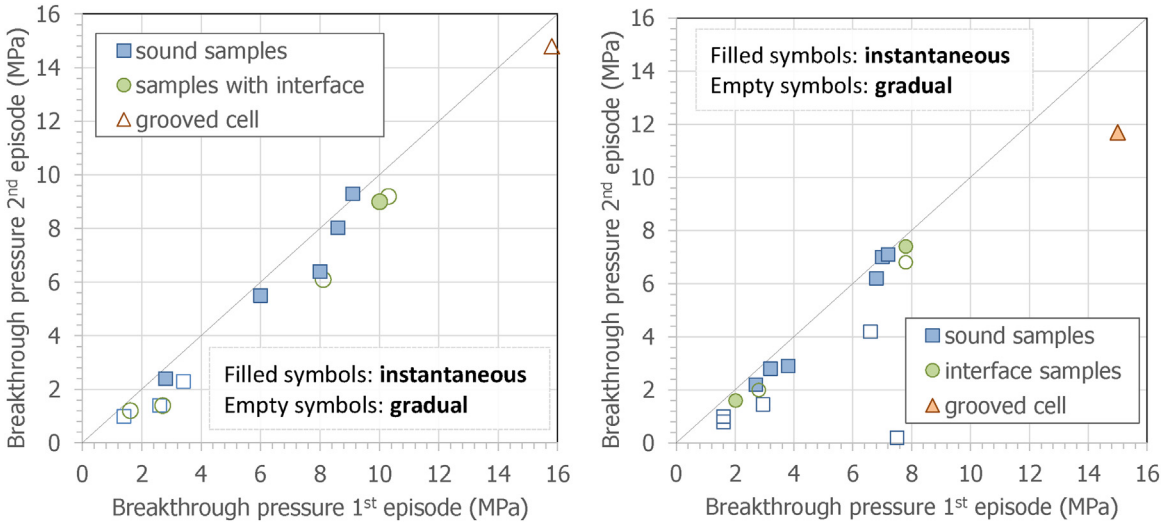

Fig. 7. Relation between the breakthrough pressures of the first and second episodes in Phase 2 (left) and Phase 4 (right).

Gradual episodes led to a decrease in the breakthrough pressure over successive episodes in the same Phase. This behaviour points to a certain weakening of the microstructure occurred as a result of the first breakthrough, but it is also probably related to the drying that the sample might have experienced as a consequence of gas flow over long time periods (see below in section 3.5). Fig. 7 shows that the reduction of breakthrough pressure of the second episode with respect to the first one was more notable in gradual episodes.

Instantaneous episodes showed high gas flow rates during a shorter period of time, revealing more robust connections, resulting in some cases in residual pressures close to zero, particularly if the dry density of the sample, and consequently swelling pressure, was low. They took place both in sound samples and in samples

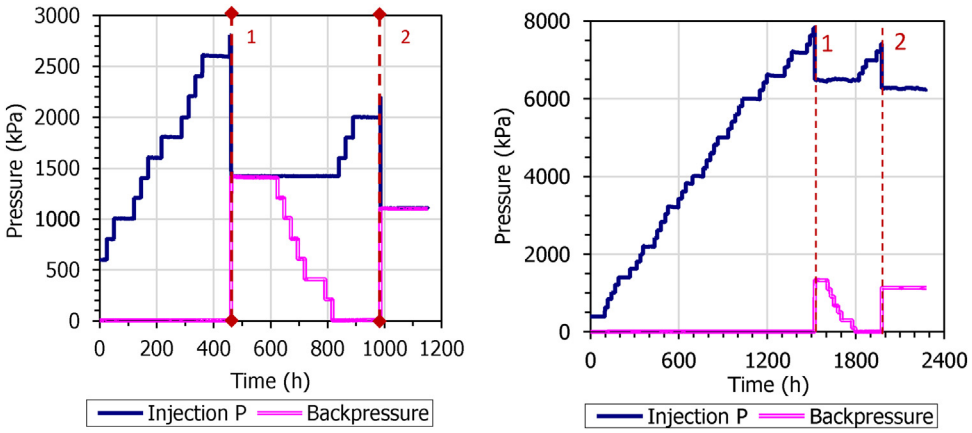

Fig. 8. Upstream and downstream pressure evolution in two subsequent breakthrough episodes during Phase 4 of a sound sample (test BT1.3_38, left) and a sample with interface (test JB1.8_38, right).

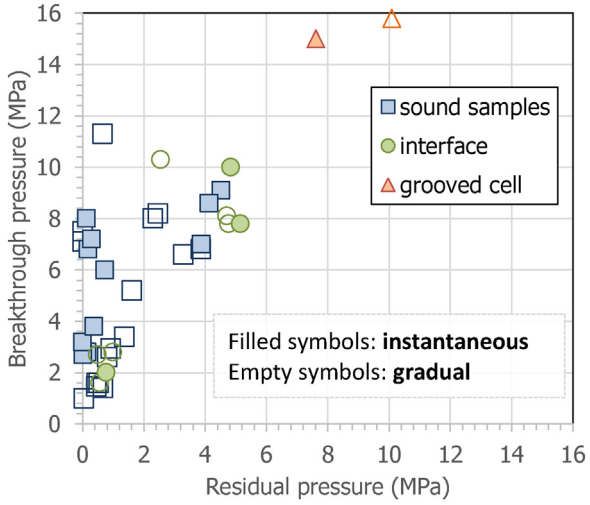

Fig. 9. Breakthrough pressure against subsequent residual pressure obtained in Phases 2 and 4 of all the tests (only first breakthrough episodes).

with interface (Fig. 8). When a breakthrough episode was forced after such instantaneous episodes, the new value of the breakthrough pressure was usually similar or only slightly lower than the last one (Fig. 7), which would indicate that the medium kept a higher integrity after gas suddenly crossed the sample than when it crossed the sample during a longer time period (gradual episodes). Instantaneous episodes could be followed by gradual episodes, but not the other way round.

Fig. 9 shows the relation between breakthrough pressure and subsequent residual pressure for all the samples tested. The results have been grouped according to the kind of breakthrough (gradual, instantaneous). The main trend was for the residual pressure to increase as breakthrough pressure was higher. In the case of sound samples, most residual pressures close to 0 corresponded to instantaneous breakthrough episodes. In contrast, this was not so clear for the samples with interface, which also tended to show higher residual pressures than sound samples. This could be caused by a higher volume of gas trapped in the samples with interface during breakthrough, but also because they were in the upper range of the densities tested (see next section for the relationship between breakthrough pressure and density). The highest breakthrough and residual pressures were measured in the sample tested in the grooved cell, which was partly caused by the higher dry density of this sample (1.61 g/cm^3) with respect to the rest of samples tested.

Fig. 10 shows the relation between the residual pressure after the first breakthrough episode of each test and the subsequent one, both in Phases 2 and 4. The results have been grouped according to the kind of samples but also to the kind of the first breakthrough episode, gradual or instantaneous. Since the residual pressures were linked to the breakthrough pressures (Fig. 9), they also tended to be higher as the dry density was higher. Gradual episodes were related to residual pressures that were very similar after the two subsequent breakthrough episodes. In contrast, after an initial instantaneous breakthrough episode, the residual pressure was lower than the one after the subsequent episode. This would mean that gas flow stopped for higher pressure gradients if the sample had experienced previously an instantaneous gas breakthrough. These trends were clearer in Phase 2, whereas in Phase 4 the residual pressures after the two subsequent breakthrough episodes were similar in all the tests, both in sound samples and in samples with interface, irrespective of the kind of breakthrough.

3.2. Relation of breakthrough pressure with swelling pressure

Fig. 11 shows the breakthrough pressures measured in the first episodes of Phases 2 and 4 as a function of the overall sample dry density determined after these phases. The breakthrough pressure increased with dry density. The Figure also shows the empirical correlation between swelling pressure and dry density for the reference FEBEX bentonite obtained with Eq. 3. The breakthrough pressure increased exponentially with dry density and was always higher than the swelling pressure corresponding to the same dry density (Gutiérrez-Rodrigo et al., 2015).

The relation between breakthrough pressure (P_b, MPa) and dry density (ρ_d, g/cm^3) in sound samples could be fitted to the following empirical expression (Gutiérrez-Rodrigo, 2018):

$$\ln P_b = 8.56\rho_d - 10.82 (28 \text{samples}, R^2 = 0.88) \quad (8)$$

Additionally, a linear relation between swelling pressure (P_s, MPa) and breakthrough pressure (MPa) was obtained:

$$P_b = 2.19 P_s - 0.43 (28 \text{samples}, R^2 = 0.85) \quad (9)$$

The samples with interface fit well in these correlations, although one of the higher density ones displayed lower breakthrough pressures than expected according to these fittings.

The results obtained in the grooved cell have also been included in the Figures. Given the high dry density of this particular sample (1.61 g/cm^3) with respect to the other samples, its breakthrough pressure was very high, but followed the same trend as the other samples with respect to dry density. However, the breakthrough

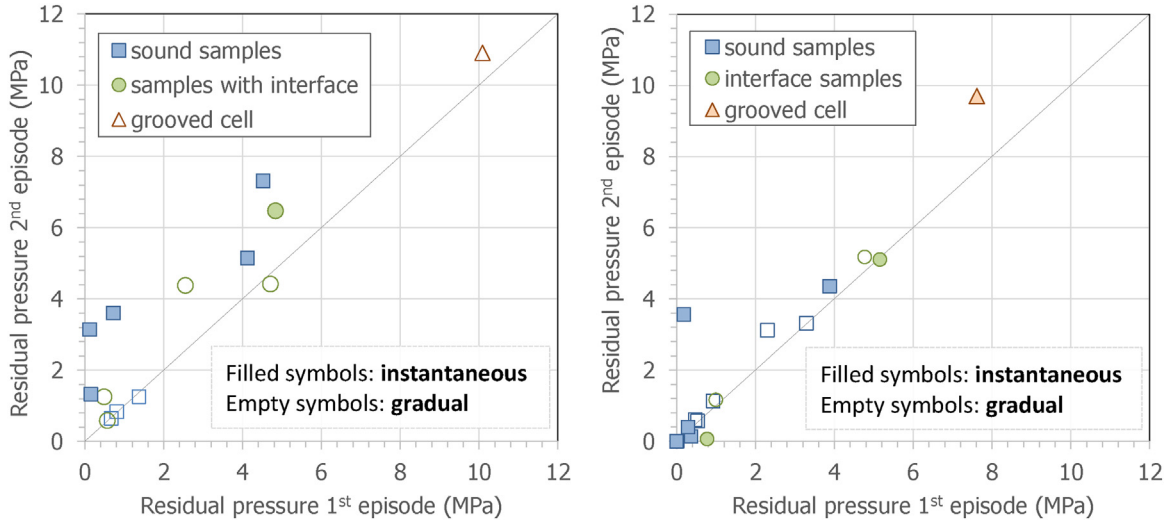

Fig. 10. Residual pressure after subsequent breakthrough episodes measured in Phase 2 (left) and Phase 4 (right).

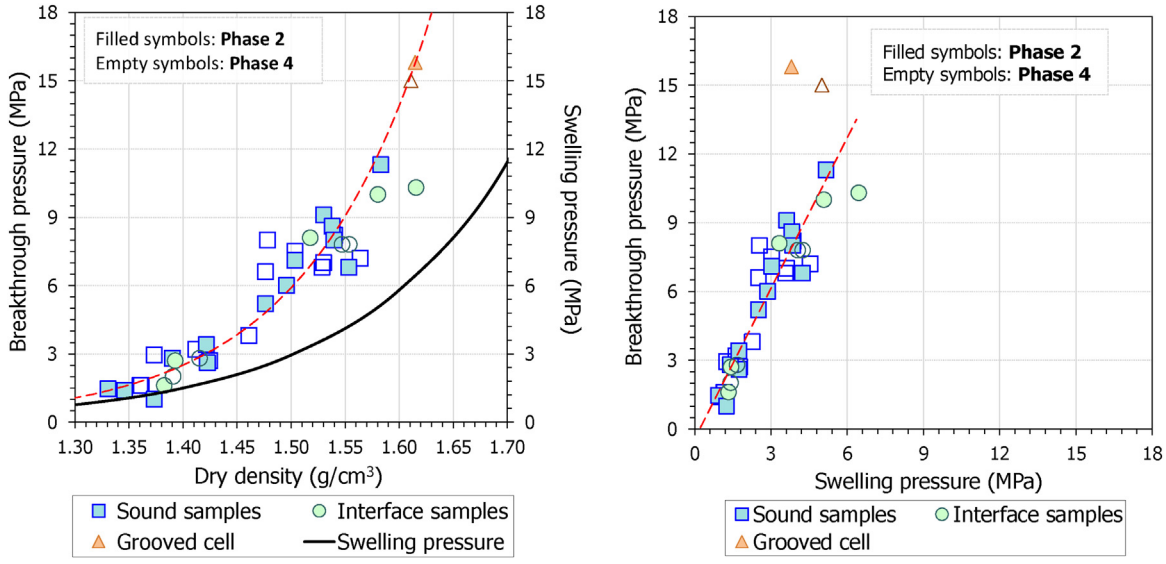

Fig. 11. Breakthrough pressure as a function of dry density (left) and of swelling pressure (right).

pressure measured was much higher than predicted with Eq. 9. This prediction was based on the results obtained in sound samples using smooth inner surface cells. The difference between those samples and the sample tested in the grooved cell could mean that in the tests performed in smooth surface cells gas could find an additional path to flow along the sample/steel interface, even though the bentonite swelling pressure would also impose a limitation for this gas flow, as attested by the increase of breakthrough pressure with swelling pressure. If this interpretation were right, the breakthrough pressure values determined could be underestimated, because of the non-discardable contribution of the bentonite/cell surface to gas flow.

3.3. Healing after resaturation

It is remarkable that the breakthrough pressure values obtained in Phases 2 and 4 were very similar. Fig. 12, in which the values obtained in the first episode before and after resaturation for each sample are plotted, highlights that after resaturation similar or slightly higher breakthrough pressure values were found if the initial breakthrough pressure was lower than 8 MPa. In some cases the increase in breakthrough pressure after resaturation could be explained by a slight increase in dry density occurred during testing (see section 3.5). This increase in dry density could only take place by sample height contraction resulting from gas pressure, which would in turn tighten the sample/cell contact around the diameter. The breakthrough pressure values higher than 8 MPa corresponded to samples of dry densities higher than 1.51 g/cm^3. Out of these samples, only in two cases (symbols inside circles in Fig. 12) there was a decrease in dry density during Phase 3 caused by the high swelling of the samples, which made difficult to keep constant volume during resaturation. In one of these samples, the decrease of breakthrough pressure in Phase 4 could be justified by the lower dry density. The behaviour of samples with and without interfaces followed the same trends. This would mean that whatever the damage caused to the microstructure during Phase 2 (reflected in the decrease of breakthrough pressure for subsequent episodes, Fig. 6), a complete healing of gas pathways took place after resaturation, and that the interface was not a preferential gas pathway after an initial breakthrough episode.

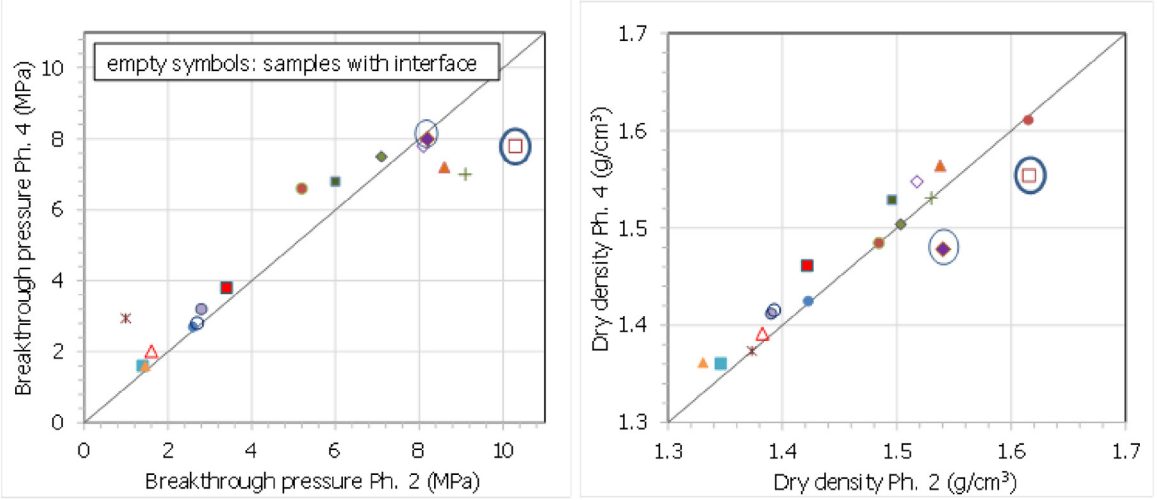

Fig. 12. Breakthrough pressures and dry densities measured for a given sample in the first episode of Phase 2 and Phase 4 (after resaturation). The symbols used for each sample are the same in both graphs.

3.4. Gas and water permeability

The pressure changes over time in both upstream and downstream cylinders after gradual breakthrough episodes were used to compute permeability values using the two-phase flow model equations for gas transport (Gutiérrez-Rodrigo et al., 2015). The equation used (Eq. 7) computes the effective permeability to gas, $k_{ig}{\cdot}k_{rg}$, where k_{ig} is the intrinsic permeability measured with nitrogen gas and k_{rg} is the relative permeability to gas. Figs. 4–6 show examples of the permeabilities computed from the pressure changes in the cylinders after breakthrough. After instantaneous breakthrough episodes the flow rate was so high, that computing permeability from it had no physical meaning.

The permeability values computed were just an approximation, because some of the required conditions to apply this equation were not completely fulfilled, like the ones needed to apply Darcy's law (because transitory or even turbulent flow can take place after the breakthrough episode). Another factor that restricted the applicability of these equations to compute permeability in these tests was that very likely flow did not make use of all the sample section (because most pores were completely saturated,) but only of preferential pathways. Nevertheless, the values obtained may allow to define some qualitative trends.

Overall the permeability computed decreased as the tests went on and gas was transferred from the upstream to the downstream cylinders. The gas transfer resulted in decreasing differential pressures and also caused a decrease in the maximum pressure applied to the sample, which would cause closing of trajectories available for gas passage as a result of the effective stress decrease. In a few tests (e.g. BT15_50 in Fig. 6), permeability kept constant for a long time and eventually increased. This behaviour was associated to null residual pressures after gradual breakthrough, which indicates that some of the trajectories opened during breakthrough remained open or were enlarged. This may have been favoured by the slight drying resulting from gas flow for long time periods (in this particular sample, the water content after Phase 2 decreased from 30.5 to 29.2%).

The effective permeability values obtained after all the gradual episodes in Phases 2 and 4 are plotted in Fig. 13 as a function of the dry density of the samples at the end of the phase, grouped by breakthrough episode. In the first episodes there was not a clear relation between permeability and dry density, which seems to confirm that gas did not flow through the sample initial porosity, but through trajectories suddenly opened. In contrast, after the second episode, the trend for the effective permeability to decrease as dry density increased seems clear. Furthermore, effective permeability after second breakthrough episodes was generally lower than after the first breakthrough for all kinds of samples. This points to a change in the gas transport mechanism, with a higher contribution of two-phase flow after the second breakthrough. As explained in section 3.1, the breakthrough pressure for the second episode was usually lower than after the first episode, which may have made more difficult the creation of new, sudden trajectories allowing a higher flow as it happened after the first episodes. In contrast, the second episodes would correspond to a gas flow more related to effective porosity (two-phase flow), being lower as the porosity was lower. In fact, after the second breakthrough an exponential relation between permeability and dry density could be defined (drawn in the Figure). In addition to their higher porosity, lower density samples develop lower swelling pressures, which would make easier the development of gas pathways. The time that gas flowed was usually shorter after the first breakthrough than after the second one.

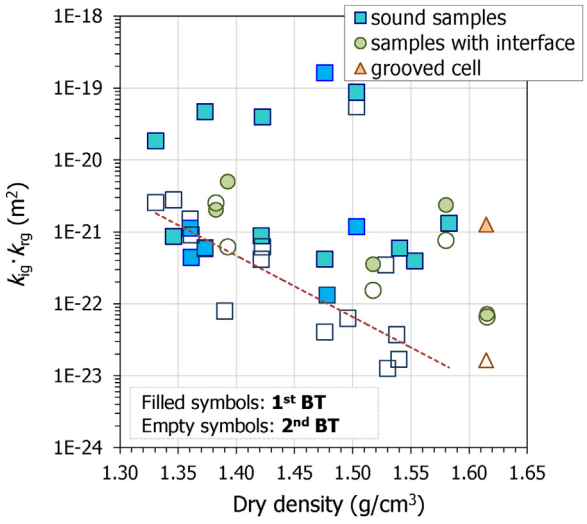

Fig. 13. Effective permeability as a function of final dry density of the samples, computed after successive breakthrough episodes of Phases 2 and 4.

In any case, the tentative gas permeabilities computed were orders of magnitude lower than those obtained for FEBEX unsat-

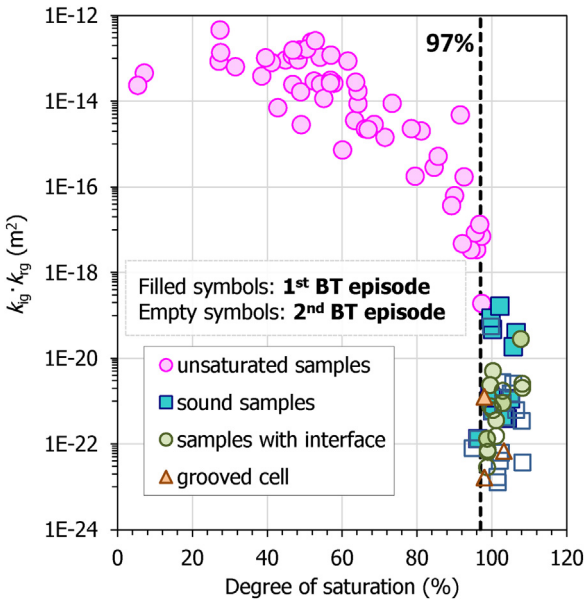

Fig. 14. Effective gas permeability as a function of degree of saturation, computed after successive breakthrough episodes of Phases 2 and 4. The values obtained in previous researches for unsaturated FEBEX samples are also included. Degrees of saturation computed using a water density of 1 g/cm^3.

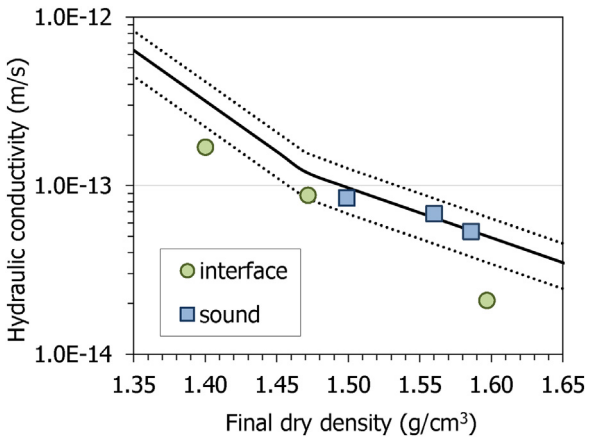

Fig. 15. Hydraulic conductivity measured at the end of the saturation phases as a function of the bentonite dry density. The empirical correlations for the reference FEBEX bentonite (Eq. 1 and 2) and their expected range of deviation (30 %) are plotted as straight lines.

urated samples of different dry density (values reported in Villar et al., 2013; Gutiérrez-Rodrigo et al., 2015; Gutiérrez-Rodrigo, 2018). These values have been plotted in Fig. 14 along with the values obtained after breakthrough commented above. In both cases the results correspond to samples compacted to different dry densities. For the unsaturated samples, the trend for effective permeability to decrease as the degree of saturation increased was very clear (related to Eq. 4). However, despite the fact that the values obtained after breakthrough corresponded all to fully saturated samples, they spanned over a broad range (between 10^{-19} to 10^{-23} m^2), which would show that porosity was not the factor controlling these tentative gas permeability values. The Figure highlights the fact that the degrees of saturation computed were mostly above 100 %, which is a consequence of using in the computation the customary value for water density of 1 g/cm^3, which is lower than the actual density of the adsorbed water in highly compacted bentonites (see for example the discussion about the topic in Jacinto et al., 2012).

In a few tests, after the resaturation Phases 1 and 3, the hydraulic conductivity of the samples was measured. Hydraulic gradients were applied between both ends of the stainless steel cells and the water outflow was measured over time (Gutiérrez-Rodrigo, 2018). As for saturation, deionised water was used, and the hydraulic gradients applied were between 600 and 7300. Usually two or three different hydraulic gradients were applied to the same sample and the permeability values plotted in Fig. 15 are the average of all of them, since they were not affected by the gradient. The hydraulic conductivity values are plotted as a function of the dry density at the end of the corresponding saturation phase, along with the range of variation of the values expected for the reference FEBEX bentonite determined with Equations 1 and 2. The results obtained in the samples that did not have an interface (sound samples) fall inside the expected range of variation. However, the samples with interface had hydraulic conductivity lower than expected. No reason has been found for this behaviour, but at least the result would confirm that the interfaces were completely sealed after saturation.

The intrinsic permeabilities corresponding to these hydraulic conductivities (computed taking into account the density and kinematic viscosity of water), were higher than the gas permeability values obtained after breakthrough shown in Fig. 14 (or obtained with Eq. 5). This would confirm that gas flow after breakthrough did not take place using all the available pore volume.

3.5. Changes in the properties of the samples during the tests

Each time a sample changed of phase, i.e. when it was moved from saturation to the breakthrough setup and backwards, it was weighed and its height was measured (without removing it from the testing cell). This allowed to estimate intermediate values of water content and dry density. At the end of Phase 1 the samples were fully saturated and in many cases, particularly if the initial dry density was high, their dry densities had decreased because of the slight axial deformation allowed by the geotextiles placed on top and bottom of the samples as hydration interface. Later, during the breakthrough phase, the samples of dry density lower than ~1.44 g/cm^3 consolidated because of the high gas pressures applied, whereas those of higher dry density could expand during the breakthrough test. The water content of all the samples tended to decrease during the breakthrough test. This decrease in water content was of between 0.05 and 3.11 % for sound samples and on average of 0.8 ± 0.7 % in samples with interface. This decrease completely recovered during resaturation in Phase 3.

At the end of the tests, the samples were extracted from the cells and subsampled to determine water content, dry density and pore size distribution (Gutiérrez-Rodrigo, 2018). In most samples, the upper section –from which gas was injected–, was slightly drier than the rest of the sample (0.3–1.7 %). The water content of subsamples taken from the external part of the bentonite cylinders, in contact with the cell wall, and from the inner part were also determined, with the aim of checking if the interface between bentonite and steel was a preferential pathway for gas flow. No significant differences were found.

In the case of samples with interface, subsamples were taken from along the interface and from parts of the bentonite sample away from the interface. After saturation the original interface was difficult to tell apart, because it appeared completely sealed (Fig. 16). The differences in the water contents and dry densities of both kinds of subsamples were not relevant and did not present any particular trend (except for sample JB1.6_38, in which a lot of material was lost during the preparation of the interface, which was very open, Fig. 17. In this case the final dry density along the interface was lower).

Fig. 16. Appearance of sample JB19_38 inside the cell before starting testing (left) and after saturation in Phase 1 (right).

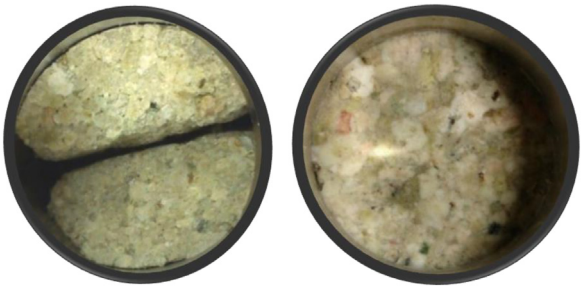

Fig. 17. Appearance of sample JB16_38 inside the cell before starting testing (left) and after saturation in Phase 1 (right).

4. Discussion

A series of tests has been presented in which saturated samples, confined in isochoric cylindrical cells, were subjected to progressively higher nitrogen gas pressures on top until gas crossed the sample and went out through its bottom. During the tests the system was a closed one, since the sample ends were connected to hermetic gas cylinders. No water supply took place during gas testing, and the gas pressure increments were performed every 24 h, to avoid significant contribution of diffusion. The gas pressure difference between the sample top and bottom cylinders at the moment of gas breakthrough has been considered the breakthrough pressure and the pressure difference between both cylinders once the gas flow through the sample stopped, the residual pressure. In a single test, breakthrough was forced twice, by appropriately changing the upstream or downstream pressures. Hence, in each test two breakthrough episodes were triggered without changing the sample conditions between them.

Gas breakthrough took place either in a sudden or in a gradual way. In the first case, i.e. in the instantaneous episodes, gas flow occurred for less than 1 h, until the upstream cylinder was emptied or the residual pressure was reached. In the gradual episodes gas flow could be prolonged over several months (usually five months). Hence, the flow rate was much lower in the gradual episodes than in the instantaneous ones (on average 3600 times higher).

After the first breakthrough episode, the subsequent breakthrough pressure was usually lower (in all cases less than 0.5 % lower), with a higher difference between both pressures (first and second) if the initial breakthrough episode had been gradual (Fig. 7). In contrast, the residual pressure after the second breakthrough episode tended to be the higher, particularly if the first episode had been instantaneous (Fig. 10). This would be caused by the progressive hydromechanical weakening of the sample (partial local desaturation resulting in a decrease of cohesion), the main mechanism being the local water transfer from higher-size pores and throats to lower-size ones. Dridi et al. (2012) considered that this behaviour could be related to the partial desaturation of the sample and/or to the incomplete cicatrisation of the preferential pathways opened during the previous breakthrough episodes. The trapping of gas bubbles during gas transport, which would allow for a better connectivity from one end to the other, would explain the higher residual pressures after the second breakthrough. In fact, the residual pressure, also known as 'capillary threshold pressure', can be considered as the minimum pressure with which gas can remain mobile within the clay (Graham et al., 2016). These processes would make easier both the opening (lower breakthrough pressure because of the large dry pores) and closure (higher residual pressure because the small pores remained saturated) of the next episode. However, the time gas flow took place after breakthrough was longer after the second episode (Gutiérrez-Rodrigo, 2018). Nonetheless, the pressure needed to establish again gas flow was still high, which shows how effectively bentonite sealed after gas went through it, even with no resaturation.

It is assumed that in gradual episodes low flow took place through small-diameter stable pathways and the gas transport mechanism was pathway dilation with modification of the local media and slow kinetics. In contrast, when instantaneous episodes took place, processes that do not correspond to the classic viscous model generated a fast gas flow. Larger and fewer pathways were very likely opened in a more mechanical way without damaging the bentonite structure, like micro-fracturing without modification of the media, i.e. a fragile failure inside the bentonite elastic field without water displacement. For this reason, the breakthrough pressure for episodes occurred after a first instantaneous breakthrough was only slightly lower than the initial one (Fig. 7). This was also found in the samples with interface, which would indicate that a saturated interface was not a preferential gas pathway after an initial breakthrough episode. A gradual episode could take place after an instantaneous episode, but not the other way round, probably because the microstructure was more damaged after a long, gradual episode, which was reflected in the decrease of breakthrough pressure after a gradual breakthrough episode.

The water content variations observed after breakthrough episodes would be lower in the case of mechanical opening processes (fracturing) and pathway dilation, whereas the higher changes would be associated with displacement of water by the gas (implying a two-phase flow, which is quite uncommon in this kind of materials) (Push and Forsberg 1983, Harrington and Horseman, 1999). In the cases where internal water redistribution with no global water content decrease happened (see section 3.5), non-noticeable microscopic two-phase flow, capable of creating gas pathways must have taken place (Volckaert et al., 1995; Ortiz et al., 2002).

The same series of tests presented in this paper were analysed by Gutiérrez-Rodrigo (2018), who checked that the size of the samples tested had influence on the results obtained. Breakthrough pressures tended to be higher in long samples, especially if their density was high. The reason would be that the longer the sample height, the lower the probability of gas pathways aperture, because of the lower pressure gradient and the larger porous structure tortuosity (which in turn depends on dry density and saturation state). Hence, the sample height would condition the actual gas pathway.

The scale effect on the results obtained was also identified by Gallé and Tanai (1998), who measured higher breakthrough pressure in a 4-cm long sample than in a 1-cm long one (>9.3 *vs.* 4.2 MPa), both of FoCa bentonite compacted to dry density of 1.6 g/cm^3. These authors also warned about the possible influence of the duration of the pressure steps on the breakthrough pressure values obtained (shorter steps would trigger higher breakthrough pressures), which is a concern also expressed by Graham et al. (2002), who considered that long duration steps would require lower pressures. Since the steps applied in the tests presented here were quite short (<24 h), the breakthrough pressure values obtained could have resulted lower if the same pressure had been kept for longer.

All the observations reported above seem to confirm that the gas transport mechanism in saturated bentonite would be microscopic pathway dilation. In contrast, for degrees of saturation lower than 97 %, previous laboratory studies showed that gas migration in FEBEX compacted bentonite under isochoric conditions would involve two-phase flow without significant deformation of the pore space (Villar et al., 2013; Gutiérrez-Rodrigo et al., 2014, 2015).

The trends commented above were also found in the samples with interface. In those samples the residual pressure for a given dry density tended to be higher than in sound samples. This could indicate that a higher volume of gas was trapped in the samples with interface during breakthrough. However, the interfaces did not seem to be weakness points in the system since this part of the samples did not generally get dryer after the tests. Popp et al. (2014) studied bentonite/sand mixtures (60/40 ratio) compacted in the shape of blocks. They analysed the behaviour of the interfaces between blocks and concluded that these interfaces were not preferential gas pathways, since the breakthrough pressure values obtained in samples with and without interface were the same, which was interpreted as an evidence of interface healing. The breakthrough pressure values found were higher than swelling pressure and related to the samples' dry density. From shear strength tests they concluded that saturation caused a strong cohesion between the matrix grains giving place to perfect healing between the sides of the interface.

Other authors observed in saturated bentonites and mixtures of bentonite and sand that the breakthrough pressure depended on dry density and was similar or slightly higher than the swelling pressure (Tanai et al., 1997; Horseman et al., 1999; Liu et al., 2014; Popp et al., 2014). The breakthrough pressure values measured in this work increased exponentially with dry density and were always considerably higher than the swelling pressure corresponding to the same dry density (Eq. 3 *vs*. Eq. 8, Villar et al., 2013; Gutiérrez-Rodrigo et al., 2015). This would mean that the swelling pressure developed by the saturated bentonite is the main mechanism hindering gas transport and suggests that flow did not occur preferentially along the interface between the sample and the cell wall (side-wall effect). In fact, the high swelling developed by the bentonite was considered a warranty of no gas flow along the interface. However, the breakthrough pressure seemed to be lower than the gas pressure required for fracturing (macroscopically) the material, since the samples were intact when the cells were dismantled. The question of the role of the cell/sample interface on overall gas transport is always a matter of concern in laboratory tests (e.g. Liu et al., 2014). To analyse this aspect one of the tests was performed in a cell whose internal wall was grooved, in opposition to the smooth inner surface of the rest of the cells. Although the relation between swelling pressure and dry density for the sample tested in the grooved cell followed the same trend as for the other samples, the breakthrough pressure measured was much higher than expected according to the linear relation established with swelling pressure for the rest of the tests (Eq. 9). This could mean that the breakthrough pressure values determined in smooth-surface cells could be underestimated, because of the contribution of the bentonite/cell interface to gas flow. Nevertheless, it seems clear that this interface did not contribute predominantly to gas flow. The extremely low permeability values measured after breakthrough (Fig. 14), lower than the water permeability corresponding to the same dry density, do neither suggest the existence of easy preferential pathways. Furthermore, no differences were found between the water contents in the parts of the samples close to the wall and in the middle of them (section 3.5), which could be an indication that no significant gas flow took place along the cell wall, because in that case some drying would have taken place.

The fact that no water pressure was applied during the breakthrough tests could mean that the breakthrough pressures in cases where the water pore pressure is higher (such as the actual state in an engineered barrier) would be even higher than those measured in this work. In this sense, Graham et al. (2016) found in their laboratory tests performed under high pore water pressure evidence indicating the potential for gas entry to occur as a result of declining pore water pressure in a repository environment.

After the samples had experienced two breakthrough episodes (Phase 2), they were resaturated for at least two months and then tested again for gas breakthrough (Phase 4). The breakthrough pressure values after resaturation, both in sound samples and in those with an interface, were similar or even higher than those found the first time the samples were tested. This would mean that whatever the damage caused to the microstructure during Phase 2, a complete healing of gas pathways and the recovering of the bentonite hydromechanical properties took place during resaturation. In a few cases, the hydraulic conductivity of the samples was measured after resaturation and before the next breakthrough test. The values obtained were in the range of those expected for the untreated reference bentonite (Eq. 1 and 2), and even lower for the samples with interface (Fig. 15). This is an additional evidence of the healing of gas pathways after resaturation and also of the initial open interfaces. Popp et al. (2014) measured the hydraulic conductivity of bentonite/sand (60/40) blocks with an interface between them and concluded that water flow took place through the matrix and not along the interface.

The gradual change of gas pressure in the cylinders connected to the samples' ends, allowed to compute tentative permeability values under the supposition of viscous flow. After the first breakthrough episodes there was not a clear relation between the effective permeability computed and the sample dry density, which seems to confirm that gas did not flow through the sample initial porosity, but through trajectories suddenly opened, which sometimes closed quickly after breakthrough and others remained open allowing a gradual decrease of gas flow. In contrast, after the second episodes, there was a trend for the effective permeability to decrease as the dry density increased (Fig. 12). This would indicate that, once the material had suffered certain local weakening and/or desaturation, the affected bentonite matrix and its swelling conditioned the easiness of the path's formation. In all cases these tentative effective gas permeabilities were much lower than the intrinsic permeabilities corresponding to the hydraulic conductivities mentioned in the previous paragraph, which would be further proof that gas flow after breakthrough did not take place using all the available sample pore volume or along the sample/cell interface.

5. Conclusions

The experimental research reported aimed at increasing the understanding of gas transport in saturated compacted bentonite used as engineered barrier in radioactive waste repositories. An engineered barrier may consist of compacted blocks and the interfaces between these could represent preferential pathways for gas flow, hence the effect of the interfaces on the gas transport was also analysed. Prior to the gas injection tests the samples were saturated, to simulate later stages of the repository life, when gas generation may be significant. As a result of the full saturation, gas was not able to flow through the samples until a sufficient pressure was reached. This breakthrough pressure was found to increase with dry density in an exponential way and was in all cases higher than the swelling pressure corresponding to the dry density of the samples. The gas breakthrough could take place either in an instantaneous or in a gradual way, the difference between both modes being the flow rate, much higher in the first case. Flow went on until the residual pressure was reached, what is interpreted as the closing of the pathways. Upon again increasing the pressure gradient, a slightly

lower gradient was necessary for flow to resume, likely as a consequence of the local hydromechanical weakening and slight local desaturation of the porous structure during the first episode. Nevertheless, the pressures needed for the second gas breakthrough episode were still much higher than the swelling pressure. The gas transport mechanism would be microscopic pathway dilation, with microfracturing in the case of the instantaneous episodes.

The samples were resaturated and the breakthrough pressures found tended to be higher (but of the same order) than before resaturation, with smaller differences between the pressures needed for first and second episodes. The hydraulic conductivity of samples that had been submitted to gas injection were in the order or even lower than that expected for the reference bentonite. These observations attest the perfect healing of previous gas pathways brought about by resaturation.

Once saturated, the samples with an interface between bentonite blocks behaved as samples of the same dry density with no interface. Hence, a sealed interface along the bentonite had no effect on the breakthrough pressure values and did not seem to be a preferential pathway after material homogenization.

The results presented allow to presume that, once the engineered barrier of an underground repository be saturated, gas pressures higher than the swelling pressure of the bentonite would have to build up before gas can move away and once this occurs, gas would not displace water. Since in the tests reported the gas pressure increase took place at a high rate, it is likely that in the real case gas could flow for lower pressures if they are sustained for longer periods of time, which would also allow for the contribution of diffusion to gas transport (negligible in these laboratory tests). In contrast, some boundary conditions of these tests have probably led to the determination of breakthrough pressure values conservative with respect to the actual conditions in a saturated engineered barrier: the samples were small, no water pressure was applied during the gas injection tests and a certain contribution of the bentonite/cell interface to gas flow could not be ruled out, even though it would be small.

The set of results presented is the first one reporting bentonite breakthrough pressures for a whole range of densities relevant for the engineered barrier of a radioactive waste repository. To the authors' knowledge it is also the first investigation on the effect of interfaces between bentonite blocks on gas transport.

CRediT authorship contribution statement

Vanesa Gutiérrez-Rodrigo: Investigation, Formal analysis, Resources, Visualization. **Pedro Luis Martín:** Conceptualization, Methodology, Formal analysis. **María Victoria Villar:** Conceptualization, Investigation, Writing - review & editing, Supervision.

Declaration of Competing Interest

The authors declare that they have no known competing financial interests or personal relationships that could have appeared to influence the work reported in this paper.

Acknowledgements

The research leading to the results presented here received funding from the European Atomic Energy Community's Seventh Framework Programme (FP7/2007–2011) under Grant Agreement No. 230 357, the FORGE project. The preparation of this paper was performed in the framework of the European Union's Horizon 2020 Research and Innovation Programme, grant agreement No <GN3>847593<GN3>. Part of the laboratory work was performed by R. Campos, J. Aroz and F.J. Romero. V. Gutiérrez-Rodrigo had a grant for research personnel training from CIEMAT.

References

Chapman, N., McCombie, C., 2003. Principles and standards for the disposal of long-lived radioactive wastes. In: Waste Management Series 3. Elsevier, Amsterdam, pp. 270.

Cuadros, J., 2008. Clays as sealing materials in nuclear waste repositories. Geol. Today 24 (3), 99–103.

Davies, C., Bernier, F., 2004. Impact of the excavation disturbed or damaged zone (EDZ) on the performance of radioactive waste geological repositories. In: Proc., European Commission CLUSTER Conference and Workshop Luxembourg, Luxembourg: European Commission, EUR 21028 EN 333 pp.

Davy, C.A., Skoczylas, F., Lebon, P., Dubois, T., 2009. Gas migration properties through a bentonite/argillite interface. Appl. Clay Sci. 42, 639–648.

Dridi, W., Gatabin, C., Guillot, W., 2012. Etude des transferts de gaz dans la bentonite FT BENTOGAZ. In: Note Technique CEA/DEN. DPC/SECR/NT/2012/047 Indice a., pp. 26.

ENRESA, 1995. Almacenamiento geológico profundo de residuos radiactivos de alta actividad (AGP). In: Diseños conceptuales genéricos. Publicación Técnica ENRESA 11/95, Madrid, pp. 105.

Ewing, R.C., Whittleston, R.A., Yardley, B.W.D., 2016. Geological disposal of nuclear waste: a primer. Elements 12, 233–237, http://dx.doi.org/10.2113/gselements.12.4.233.

Gallé, C., 2000. Gas breakthrough pressure in compacted Fo-Ca clay and interfacial gas overpressures in waste disposal context based materials. Appl. Clay Sci. 17, 85–97.

Gallé, C., Tanai, K., 1998. Evaluation of gas transport properties of backfill materials for waste disposal: H_2 migration experiments in compacted Fo-Ca clay. Clays Clay Miner. 46 (5), 498–508.

Gens, A., Garitte, B., Olivella, S., Vaunat, J., 2009. Applications of multiphysical geomechanics in underground nuclear waste storage. Eur. J. Env. Civil Engng. 13 (7–8), 937–962.

González-Blanco, L., Romero, E., Jommi, C., Sillen, X., Li, X., 2017. Exploring fissure opening and their connectivity in a Cenozoic clay during gas injection. In: Ferrari, A., Laloui, L. (Eds.), Advances in Laboratory Testing and Modelling of Soils and Shales (ATMSS). Springer Series in Geomechanics and Geoengineering. Springer, Cham, Switzerland, pp. 288–295, http://dx.doi.org/10.1007/978-3-319-52773-4-33, ISBN 978-3-319-52772-7.

Graham, J., Halayko, K.G., Hume, H., Kirkham, T., Gray, M., Oscarson, D., 2002. A capillarity-advective model for gas break-through in clays. Eng. Geol. 64, 273–286.

Graham, C.C., Harrington, J.F., Sellin, P., 2016. Gas migration in pre-compacted bentonite under elevated pore-water pressure conditions. Appl. Clay Sci. 132-133, 353–365, http://dx.doi.org/10.1016/j.clay.2016.06.029.

Gutiérrez-Rodrigo, V., 2018. Transporte de gas en materiales de barrera. In: Universidad Complutense de Madrid. Colección Documentos. CIEMAT, Madrid, pp. 303, Tesis Doctoral.ISBN: 978-84-7834-802-2.

Gutiérrez-Rodrigo, V., Villar, M.V., Martín, P.L., Romero, F.J., 2014. Gas transport properties of compacted bentonite. In: Khalili, N., Russell, A., Khoshghalb, A. (Eds.), Unsaturated Soils: Research and Applications, 2. Taylor & Francis Group, London, pp. 1735–1740, ISBN: 978-1-138-00150-3.

Gutiérrez-Rodrigo, V., Villar, M.V., Martín, P.L., Romero, F.J., Barcala, J.M., 2015. Gas-breakthrough pressure of FEBEX bentonite. In: Shaw, R.P. (Ed.), Gas Generation and Migration in Deep Geological Radioactive Waste Repositories, 415. Geological Society, London, Special Publications, pp. 47–57, http://dx.doi.org/10.1144/SP415.4, First published online November 14, 2014.

Harrington, J.F., Horseman, S.T., 1999. Gas transport properties of clays and mudrocks. In: Aplin, A.C., Fleet, A.J., Macquaker, J.H.S. (Eds.), Muds and Mudstones: Physical and Fluid Flow Properties, 158. Geological Society of London, Special Publication, pp. 107–124.

Harrington, J.F., Horseman, S.T., 2003. Gas migration in KBS-3 buffer bentonite: sensitivity of test parameters to experimental boundary conditions. In: Report TR-03-02. Svensk Kärbränslehantering AB (SKB), Stockholm, Sweden.

Harrington, J.F., Graham, C.C., Cuss, R.J., Norris, S., 2017. Gas network development in a precompacted bentonite experiment: evidence of generation and evolution. Appl. Clay Sci. 147, 80–89.

Horseman, S.T., Harrington, J.F., Sellin, P., 1999. Gas migration in clay barriers. Eng. Geol. 54, 139–149.

Jacinto, A., Villar, M.V., Ledesma, A., 2012. Influence of water density on the water-retention curve of expansive clays. Gotechnique 62 (8), 657–667, http://dx.doi.org/10.1680/geot.7.00127.

Johnson, L.H., 2006. Gas production and transport in the near field of SF and HLW repositories in clay and crystalline rocks: processes, uncertainties and performance assessment aspects. In: NF-PRO (Contract No F16W-CT-2003-02389) Report (deliverable D-No: 5.1.6).

Liu, J.F., 2013. In: Centrale de Lille, École (Ed.), Étanchéité de l'interface argilite-bentonite re-saturée et soumise à une pression de gaz, dans le contexte du stockage profond de déchets radioactifs. , p. 197, Ph.D.

Liu, J.F., Davy, C.A., Talandier, J., Skoczylas, F., 2014. Effect of gas pressure on the sealing efficiency of compacted bentonite-sand plugs. J. Contam. Hydrol. 170, 10–27.

Loosveldt, H., Lafhaj, Z., Skoczylas, F., 2002. Experimental study of gas and liquid permeability of a mortar. Cem. Concr. Res. 32, 1357–1363.

Olivella, S., Alonso, E.E., 2008. Gas flow through clay barriers. Gotechnique 58 (3), 157–176.

Ortiz, L., Volckaert, G., Mallants, D., 2002. Gas generation and migration in Boom Clay, a potential host rock formation for nuclear waste storage. Eng. Geol. 64, 287–296.
Popp, T., Rölke, C., Salzer, K., 2014. Hydromechanical properties of bentonite-sand block assemblies with interfaces in engineered barrier systems. In: Shaw, R.P. (Ed.), Gas Generation and Migration in Deep Geological Radioactive Waste Repositories, 415. Geological Society, London, Special Publications, pp. 19–33.
Pusch, R., 1994. Waste disposal in rock. Developments in Geotechnical Engineering, vol. 76. Elsevier, Amsterdam, pp. 490.
Pusch, R., Forsberg, T., 1983. Gas migration through bentonite clay. In: SKB Technical Report 83-71, Stockholm, Sweden.
Rodwell, W.R., Harris, A.W., Horseman, S.T., Lalieux, P., Muller, W., Ortiz Amaya, L., Pruess, K., 1999. Gas migration and two-phase flow through engineered and geological barriers for a deep repository for radioactive waste. In: A Joint ECrNEA Status Report, EUR 19122 EN. European Commission, Nuclear Energy Agency, Brussels, Luxembourg, pp. 429.
Scheidegger, A.E., 1974. The Physics of Flow through Porous Media, 3rd ed. University of Toronto Press, Toronto.
Sellin, P., Leupin, O., 2013. The use of clays as an engineered barrier in radioactive-waste management – a review. Clays Clay Miner. 61 (6), 477–498, http://dx.doi.org/10.1346/CCMN.2013.0610601.
Shaw, R.P., 2015. The fate of repository gases (FORGE) project. In: Shaw, R.P. (Ed.), Gas Generation and Migration in Deep Geological Radioactive Waste Repositories, 415. Geological Society, London, Special Publications, pp. 1–8.
Tanai, K., Kanno, T., Gallé, C., 1997. Experimental study of gaspermeabilities and breakthrough pressures in clays. 1996 December 2-6; Boston, MA In: Proc Fall Meet Material Research Society, vol 465, pp. 995–1002.
Villar, M.V., Gutiérrez-Rodrigo, V., Martín, P.L., Romero, F.J., Barcala, J.M., 2013. Gas transport in bentonite. In: Informes Técnicos CIEMAT 1301., pp. 63, http://dx.doi.org/10.13140/RG.2.2.14334.28489, Madrid.
Volckaert, G., Ortiz, L., de Cannière, P., Put, M., Horseman, S.T., Harrington, J.F., Fioravante, V., Impey, M., 1995. Modelling and experiments on gas migration in repository host rocks (MEGAS project). In: European Commission Report EUR 16235 EN., pp. 447.
Xu, L., Ye, W.M., Ye, B., Chen, B., Chen, Y.G., Cui, Y.J., 2015. Investigation on gas migration in saturated materials with low permeability. Eng. Geol. 197, 94–102.